Nat. Hazards Earth Syst. Sci. Discuss., 1, 7015–7058, 2013
www.nat-hazards-earth-syst-sci-discuss.net/1/7015/2013/
doi:10.5194/nhessd-1-7015-2013

Natural Hazards and Earth System Sciences
Open Access
Discussions

Modelling the NO emissions from wildfires at the source level

Y. Pérez-Ramirez[1], P.-A. Santoni[2], and N. Darabiha[2]

[1]UMR CNRS 6134 – SPE, University of Corsica, Corte, France
[2]Laboratoire EM2C, CNRS UPR 288, Ecole Centrale Paris, Chatenay Malabry, France

Received: 30 September 2013 – Accepted: 8 November 2013 – Published: 4 December 2013

Correspondence to: Y. Pérez-Ramirez (perez-ramirez@univ-corse.fr)

Published by Copernicus Publications on behalf of the European Geosciences Union.

Abstract

There is a growing interest to characterize fire plumes in order to control air quality during wildfire episodes and to estimate the carbon and ozone balance of fire emissions. A numerical approach has been used to study the mechanisms of NO formation at the source level in wildfires given that NO plays an important role on the formation of ground-level ozone. The major reaction mechanisms involved in NO chemistry have been identified using reactions path analysis. Accordingly, a two-step global kinetic scheme in the gas phase has been proposed herein to account for the volatile fuel-bound nitrogen (fuel-N) conversion to NO, considering that the volatile fraction of fuel-N is released as NH_3. Data from simulations using the PSR code from CHEMKIN-II package with a detailed kinetic mechanism (GDF-kin® 3.0) have been used to calibrate and evaluate the global model under typical wildfire conditions in terms of the composition of the degradation gases of vegetation, the equivalence ratio, the range of temperatures and the residence time.

1 Introduction

Wildfires are a major emission source of CO, CO_2, NO_x ($NO + NO_2$), volatile organic compounds (VOCs) and particulates to the atmosphere (Barboni et al., 2010), which in turn can form secondary pollutants with implications at local/regional scale (i.e. air quality, human health) or at global scale (i.e. climate dynamics). This is the case of NO_x which are major contributors of photochemical smog and thus of ground-level ozone (Grewe et al., 2012).

On the context of the present climate change scenario there is a growing interest to characterize fire plumes in order to control air quality during wildfire episodes and to estimate the carbon and ozone balance of fire emissions (Miranda, 2004; Strada et al., 2012).

NHESSD
1, 7015–7058, 2013

Atmospheric emissions from wildfires have generally been assessed using bottom-up estimates which require explicit knowledge on fire behaviour, area burned, fuel consumption, fuel characteristics and pollutants specific emission factors at the source level. Even though the recent improvements, these methods entail errors and uncertainties in each step (Ottomar et al., 2009), particularly concerning the emission factors. In this regard, in the literature average values of emission factors can be found for a given pollutant and vegetation structure, nevertheless there are wide variations in the values presented for the same type of vegetation; this is especially remarkable in the case of certain pollutants such as NO_x (Mebust et al., 2011). This variability underlines the generally limited understanding on the combustion processes of vegetation (Sullivan and Ball, 2012).

Average emission factors for a certain type of vegetation structure are useful to generate overall emission factors; however they do not reflect the spatial and temporal variability of wildfires. The wide range in observed emissions from a single fire reflects the variable and changing combustion conditions (Jaffe and Wigder, 2012). Thus, studies focused on understanding instantaneous emissions from wildfires require more detailed information on the emissions of pollutants at the source level and thus on the combustion processes of vegetation.

Likewise, the analysis of combustion processes is also decisive for wildfires' behaviour modelling. In fact the rate and amount of energy released from the fuel and thus the amount of energy to be transferred to surrounding unburned fuel, which may induce its subsequent ignition, are derived from the fundamental chemistry of the fuel and its combustion (Sullivan, 2009).

However, the use of detailed kinetic mechanisms, which involve a large number of chemical species and reactions, results in an unfeasible solution to predict fire spread and its associated pollutant emissions at the landscape scale. The number of chemical species and reactions included in a kinetic mechanism must be a balance of the competing needs of accuracy and simplicity to attain the computational time requirements. In this regard, global kinetic mechanisms attempt to simplify the detailed

NHESSD
1, 7015–7058, 2013

chemistry in order to predict important physical quantities, such as the concentration profile of the principal species or the rate of energy released.

The aim of this work is to improve the current knowledge on the combustion processes responsible for the emissions of pollutants of wildland fires at the source level by focusing on NO modelling. With this purpose, it has been developed a two-step global oxidation scheme to account for the NO emissions in wildland fire conditions. The major reaction mechanisms involved in NO chemistry have been identified using reactions path analysis through reactions rates analysis and sensitivity analysis with a detailed kinetic mechanism (GDF-kin® 3.0). The kinetic parameters of the global model have been determined using numerical data obtained with GDF-kin® 3.0 in a perfectly-stirred reactor environment under typical wildfire conditions in terms of the inlet mixture composition, equivalence ratio and range of temperatures. Moreover, the model has been tested in conditions other than the calibration conditions in terms of the residence time.

Section 2 is devoted to the procedures concerning the study of NO chemistry and the calibration of the global model. Next, Sect. 3 is focused on the reactions path analysis through rate-of-production and sensitivity analyses. Sections 4 and 5 concern the derivation of the global model and the evaluation of the performances of the model in comparision with experimental data available on the literature and the numerical results obtained from a detailed kinetic mechanism (GDF-kin® 3.0) for different residence times. Finally, conclusions are summarized in Sect. 6.

2 Materials and methods

2.1 Degradation gases of vegetation

The use of global kinetic mechanisms entails the simplification of not only combustion kinetics but also fuel chemistry since all the species present in the gases released from the thermal degradation of vegetation cannot be taken into account. Often, for fire

NHESSD
1, 7015–7058, 2013

modelling purposes it is generally assumed that the degradation gases of vegetation are composed only by the chemical species present in larger amounts, i.e. CO and CO_2 (Morvan and Dupuy, 2004). However, the simplification of the composition of the degradation gases mixture can lead to a loss of accuracy of the model predictions (Tihay et al., 2009a) and also the estimation of pollutants emissions as NO.

Several mechanisms can lead to the formation of NO (Glarborg, 2007). These mechanisms imply either the fixation of the molecular nitrogen contained in the combustion air (i.e. thermal, prompt, N_2O and NNH pathways) or the oxidation of organic nitrogen chemically bound in the fuel (i.e. fuel-N pathway).

In the combustion of vegetation, the main path for NO formation is the fuel-N route (Salzmann and Nussbaumer, 2001; Rogaume et al., 2006; Glarborg, 2007). Vegetation contains small amounts of fuel-bound nitrogen, typical values range from 0.1 to 3.5 % weight (Glarborg, 2007). When vegetation is exposed to a thermal source during the degradation, the parent fuel-N is partly released as volatile-N and partly transformed in char-N. The volatile fraction is essentially composed by HCN, NH_3, HNCO and tars. Some authors have reported that NH_3 is the main volatile-N species during biomass pyrolysis and that the release of HCN from the fuel was always almost negligible (Weissinger et al., 2004; Zhou et al., 2006). Nevertheless, the extent of conversion of fuel-N to NO is nearly independent of the identity of the model compound (HCN, NH_3, etc.), but is strongly dependant on the local combustion environment (temperature and stoichiometry) and on the initial level of nitrogen compound in the fuel-air mixture (Sullivan et al., 2002).

The fuel-N mechanism is more complex than the other NO formation paths and even though the overall mechanism is fairly well established details are still under investigation especially for heterogeneous mixtures due to the sensitization effects between species, such as methane or carbon oxides to nitrogen oxides (Faravelli et al., 2003; Glarborg, 2007; Mendiara and Glarborg, 2009). This is the case of the gases released from the thermal degradation of vegetation which form a mixture containing a great variety of chemical species. Indeed the complexity of the combustion processes

NHESSD
1, 7015–7058, 2013

involving the degradation gases of vegetation relies on their composition and the wide range of conditions occurring in a wildfire.

To our knowledge, there are no studies on the literature concerning the composition of the degradation gases of forest fuels quantifying the volatile fraction of fuel-N. However, Leroy et al. (2008) carried out a detailed study of the oxidation of a $CH_4/CO/CO_2$ gas mixture representative of the thermal degradation of *Pinus pinaster* needles, which is a natural species frequently used in wildfires experimentation since it is a widespread species characteristic of the forests in the Mediterranean Basin. This gaseous mixture was obtained using a tubular furnace allowing the pyrolysis of *Pinus pinaster* needles under an inert atmosphere (Tihay et al., 2009b). Experiments were conducted in the temperature range of 563–723 K, which corresponds to the maximum yields of gas released observed in thermogravimetric analysis (TGA) on thermal degradation of forest fuels.

So we considered the gaseous mixture proposed by Leroy et al. (2008) but doped with the corresponding volatile-N fraction released from the thermal degradation of the pine needles. For this, we assumed that volatile-N was only composed by NH_3 because although the nitrogen species (NH_3, HCN) initially follow different oxidation paths, the steps that determine the selectivity towards NO and N_2 are essentially the same (Sullivan et al., 2002). Then, we considered that the volatile-N fraction corresponded to 80 % of the amount of fuel bound nitrogen (Brink et al., 2001), which was obtained from an elementary analysis of a sample of *Pinus pinaster* needles. The resulting mixture composition for the degradation gases of *Pinus pinaster* needles was: 0.23 % of NH_3, 30.43 % of CO, 50.98 % of CO_2 and 18.36 % of CH_4 (mole fractions).

2.2 Numerical approach

Calculations were carried out using the PSR code (Glarborg et al., 1986) from CHEMKIN-II package (Kee et al., 1989) which provides predictions of the steady-state temperature and species composition in a perfectly-stirred reactor (PSR). In a PSR the rate of conversion from reactants to products is kinetically-controlled and therefore,

NHESSD
1, 7015–7058, 2013

combustion is only characterized by the residence time, the mixture composition and the temperature. Thus, the PSR configuration allows testing the global model at different temperatures and fuel equivalence ratios.

The global model formulation was derived from the full reaction mechanism through sensitivity analysis and rate-of-production analysis of PSR calculations covering the range of interest for the gaseous mixture previously detailed (Sect. 2.1). Only the reactions concerning species with a rate of production greater than 5 % and the reactions with sensibility greater than 5 % were considered.

Regarding the calibration of the reaction rate expressions, a regression analysis was performed whereby the global parameters were adjusted by optimizing the match between the main species (i.e. NO and NH_3) concentration profiles (as a function of the temperature and fuel equivalence ratio) obtained by the global model and the reference detailed mechanism (GDF-kin® 3.0). For this, the NO global model was coupled to a 5-steps global kinetic mechanism (Pérez-Ramirez et al., 2012) in order to take into account the combustion of the CH_4/CO present in the degradation gases of vegetation.

Simulations for the sensitivity analysis, reaction path analysis and the calibration of the model were performed at atmospheric pressure and at a constant residence time, for temperatures ranging between 773 and 1273 K (stepping 50 K) and fuel equivalence ratios between 0.6 and 1.4. Moreover, reactants were diluted in argon (dilution factor 9.2) to avoid temperature rise in the reactor.

The residence time was set at 1.3 s. This value was proposed by Jallais (2001) as an optimum value of time for controlling species to build up in a PSR of the same volume. In addition this value is in accordance with the recommendations of David and Matras (1975) to assure a homogeneous distribution of species in PSR devices.

In order to test the model in conditions other than the calibration conditions, the model was evaluated for another residence time. In this case, the residence time was set at 0.6 s. This value has been obtained from measurements performed at landscape scale in experimental fires across shrubland fuels (Santoni et al., 2006) and it corresponds to the average transit time of the degradation gases through the

NHESSD
1, 7015–7058, 2013

flame, i.e. from the base to the tip of the flame (Santoni, 2008). It is worth noting that the residence time for PSR calculations is not equivalent to the residence time of the flame, which is defined as the average time that the flame stays in a certain position and it is thus related to the rate of spread.

2.3 Reference detailed kinetic mechanism

To our knowledge, there are no experimental data in the literature concerning the NO formation in PSR devices for $CH_4/CO/CO_2/NH_3$ gases mixtures in the conditions of this study. Indeed, experimental data available in the literature is very limited and concern gas mixtures of CH_4 (Bartok et al., 1972; Duterque et al., 1981), CH_4/C_2H_6 (Dagaut et al., 1998) or other hydrocarbons such as C_3H_8, C_6H_6 and C_8H_{18} (Duterque et al., 1981) doped with different nitrogen compounds (e.g. NH_3, NO, HCN, etc.). The experimental conditions differ depending on the work and only the experiments performed by Dagaut et al. (1998) are closer to the conditions encountered in the combustion of vegetation in terms of temperature and fuel equivalence ratio. In this regard, Dagaut et al. (1998) carried out the experiments at temperatures ranging from 1100 to 1500 K and for fuel equivalence ratios in the range of 0.75–2.5. Dagaut et al. (1998) developed a detailed chemical kinetic model based on these experiments.

Thus, due to the lack of experimental data, the kinetic parameters of the reaction rate equations were fitted according to numerical results obtained with the detailed kinetic mechanism GDF-Kin® 3.0 (El Bakali et al., 2006). This mechanism developed for the oxidation of natural gas takes into account the major and the minor alkanes present in the natural gas. Moreover, it incorporates the chemistry of nitrogen oxides from the mechanism developed by Dagaut et al. (1998).

Even though GDF-Kin® 3.0 has not been specifically developed for the gas-phase combustion processes of vegetation; it has proven its performance for different test environments (e.g. shock tubes and jet-stirred reactors, premixed flames) and in

NHESSD
1, 7015–7058, 2013

various conditions of temperature, pressure and equivalence ratio (El Bakali et al., 2004, 2006).

2.4 Global kinetic mechanism for the combustion of CH_4/CO

The NO global model was implemented in conjunction with a 5-steps global mechanism (Pérez-Ramirez et al., 2012) to model the combustion of the CH_4/CO present in the degradation gases of vegetation. This mechanism was developed for the conditions encountered in a wildfire scenario and it was calibrated by using the experimental data obtained by Leroy et al. (2008) in a perfectly-stirred reactor.

The first Reaction (R1) of this mechanism describes the breakdown of methane to an intermediate species, the methyl radical. The second and third Reactions (R2 and R3), describe the subsequent oxidation of the intermediate species, the methyl radical and the formaldehyde, to carbon monoxide. And the fourth and fifth steps (Reactions R4 and R5), correspond respectively to the oxidation of hydrogen and carbon monoxide.

$$CH_4 \Rightarrow CH_3 + \frac{1}{2}H_2 \quad \text{(R1)}$$

$$CH_3 + \frac{1}{2}O_2 \Rightarrow CH_2O + \frac{1}{2}H_2 \quad \text{(R2)}$$

$$CH_2O + \frac{1}{2}O_2 \Rightarrow CO + H_2O \quad \text{(R3)}$$

$$H_2 + \frac{1}{2}O_2 \Leftrightarrow H_2O \quad \text{(R4)}$$

$$CO + \frac{1}{2}O_2 \Leftrightarrow CO_2 \quad \text{(R5)}$$

The reaction rate parameters of the CH_4/CO global model are listed in Table 1.

NHESSD
1, 7015–7058, 2013

3 Reactions analysis

3.1 Combustion of $CH_4/CO/CO_2$ mixture

The oxidation paths of $CH_4/CO/CO_2$ mixture are similar to the oxidation paths of methane as identified by Leroy et al. (2008). Two pathways for the oxidation of methane can be established (Fig. 1). The first one is direct oxidation to CH_3 which subsequently oxidizes to CH_3O and CH_2O. The second path is oxidation to CH_3 followed by the recombination of CH_3 molecules to the formation of C_2 hydrocarbons. The selectivity to one or the other pathway is given by the fuel equivalence ratio. In fuel-rich conditions the formation of C_2 hydrocarbons will be favoured whereas in fuel-lean conditions, the direct oxidation will be preferential. Consequently, a different behaviour would also be expected for the oxidation of NH_3 and thus the NO chemistry depending on the conditions in terms of the fuel equivalence ratio, as also pointed out in the literature (Sullivan et al., 2002).

3.2 NO reaction paths analysis

3.2.1 Fuel-lean conditions

Figure 2 presents the reactions paths diagram of the principal reactions involved in the NO chemistry at fuel-lean conditions which has been obtained from the results of both the rate-of-production analysis and the sensitivity analysis. As shown in Fig. 2, the oxidation of NH_3 leads to two main products, NO and N_2. According to the data obtained from the simulations with the detailed kinetic mechanisms around 23 % of NH_3 is converted to NO and 76 % is converted to N_2. The remaining amount, less than 1 %, comprises other N-compounds as NO_2 and N_2O.

Concerning the reaction paths, NH_3 is mainly converted to NH_2 by hydrogen abstraction (Reaction R6). NH_2 is then partly recycled back to NH_3, essentially by

NHESSD
1, 7015–7058, 2013

reacting with the hydroperoxyl radical (Reaction R7).

$$NH_3 + OH \Leftrightarrow NH_2 + H_2O \quad \text{(R6)}$$

$$NH_2 + HO_2 \Leftrightarrow NH_3 + O_2 \quad \text{(R7)}$$

The subsequent reactions of NH_2 largely determine the formation of N_2 or NO. Formation of N_2 occurs mostly through the reaction of NH_2 with NO (Reaction R8). This pathway accounts for 80 % of the total N_2 formation according to the results of the rate-of-production analysis.

$$NH_2 + NO \Leftrightarrow N_2 + H_2O \quad \text{(R8)}$$

NO formation occurs essentially by the oxidation of nitroxyl (Reaction R9, Fig. 3) through the sequence $NH_3 \rightarrow NH_2$ ($\rightarrow H_2NO$) $\rightarrow$ HNO $\rightarrow$ NO (Fig. 2). Thus nitroxyl can be formed directly by NH_2 or via H_2NO species. The reaction pathway involving H_2NO has been identified as being important only in the presence of high CO_2 concentrations (Mendiara and Glarborg, 2009).

$$HNO + O_2 \Leftrightarrow NO + HO_2 \quad \text{(R9)}$$

Once NO is formed, some NO to NO_2 interconversion occurs by the reaction of NO with the hydroperoxyl radical (Reaction R10).

$$NO + HO_2 \Leftrightarrow NO_2 + OH \quad \text{(R10)}$$

However, part of the NO_2 is converted back to NO directly or via HONO (Table 2). For temperatures lower than 1023 K, NO_2 reacts with CO to form NO and CO_2 (Fig. 3, Reaction R11). It worth noting that in this range of temperatures the oxidation of CO is not efficient. For temperatures higher than 1023 K, when the NO production is more efficient, NO_2 is almost entirely converted back to NO by reacting with the H and O radicals (Reactions R12 and R13, Table 2). These two reactions are fast if their activation energy is considered (i.e. 362 and 600 cal mol^{-1}, respectively). So, in the

NHESSD
1, 7015–7058, 2013

presence of high concentrations of radicals, NO_2 is rapidly converted back to NO (Miller and Bowman, 1989).

$$NO_2 + CO \Leftrightarrow NO + CO_2 \quad \text{(R11)}$$

$$NO_2 + H \Leftrightarrow NO + OH \quad \text{(R12)}$$

$$NO_2 + O \Leftrightarrow NO + O_2 \quad \text{(R13)}$$

NO is also removed to form HNO by reacting with HCO at high temperatures (Reaction R14). However, as NO_2, HNO is almost entirely converted back to NO.

$$NO + HCO \Leftrightarrow HNO + CO \quad \text{(R14)}$$

Figures 4 and 5 present the results of the sensitivity analysis at 1073 and 1273 K respectively. This range of temperatures corresponds to the more efficient NO production in the conditions of this study. In these figures, a positive sensitivity coefficient of the reaction indicates that increasing the corresponding reaction rate in a forward direction contributes to increases in NO concentrations and a negative sensitivity indicates the opposite.

The sensitivity analysis highlights how the NO chemistry strongly depends on reactions involving NH_2, the influence of the H_2NO route and the importance of the composition of the radical pool. As temperature increases, according to the results of the sensitivity analysis at 1273 K, reactions involving hydrocarbon radicals and CO become relevant in the NO chemistry.

3.2.2 Fuel-rich conditions

At fuel-rich conditions NO chemistry is more complex than at fuel-lean conditions as indicated by the reactions paths diagram presented in Fig. 6. In these conditions, the 83 % of NH_3 leads to the formation of N_2 and NO. The remaining amount of NH_3 is principally converted to HCN.

As at fuel-lean conditions, NH_3 is mainly converted to NH_2 by hydrogen abstraction (Reaction R6). Moreover, at fuel-rich conditions and temperatures higher than 1073 K,

NHESSD
1, 7015–7058, 2013

reaction with oxygen atom (Reaction R15) also provides a non-negligible contribution to NH_2 formation.

$$NH_3 + O \Leftrightarrow NH_2 + OH \quad \text{(R15)}$$

Part of NH_2 may be recycled to NH_3 by reacting with the hyrodperxyl radical (Reaction R7), as at fuel-lean conditions. However, other reactions involving NH_2 participate in the NH_3 formation (Reactions R16–R18).

$$NH_2 + H_2 \Leftrightarrow NH_3 + H \quad \text{(R16)}$$

$$NH_2 + H + M \Leftrightarrow NH_3 + M \quad \text{(R17)}$$

$$NH_2 + HNCO \Leftrightarrow NH_3 + NCO \quad \text{(R18)}$$

The subsequent reactions of NH_2 largely determine the formation of N-containing compounds since the formation of N_2, N_2O and NO mostly occur by reactions involving amine radical species.

The formation of N_2 follows essentially the same pathways than at fuel-lean conditions, this is through the reaction of NH_2 with NO (Reaction R8). In the same way, N_2O is also produced by the reaction of NH_2 with NO (Reaction R19). This reaction represents a minor contribution in NO consumption in the conditions of this study. The normalized rate-of-consumption of NO due to this reaction at 1273 K is −0.055. Moreover, N_2O is almost entirely consumed to form N_2 by reaction with CO and to a lower extend with H.

$$NH_2 + NO \Leftrightarrow N_2O + H \quad \text{(R19)}$$

Concerning NO, it is mostly produced by reactions involving HNO (Fig. 7). Between 773 and 1023 K, the oxidation of HNO (Reaction R9) is the main source of NO, but also the reactions of HNO with CO (reverse reaction Reaction R14) or the thermal dissociation of HNO (Reaction R20) contribute to the NO formation. For higher temperatures the

NHESSD
1, 7015–7058, 2013

reaction of HNO with the H radical (Reaction R21) becomes significant.

$$HNO + M \Leftrightarrow NO + H + M \quad \text{(R20)}$$

$$HNO + H \Leftrightarrow NO + H_2 \quad \text{(R21)}$$

HNO is mainly formed by NH_2 and H_2NO, but also by the isocyanic acid (HNCO) due to the reaction NH_2 + CO. The presence of CO in the degradation gases of vegetation enhances this reaction. However, this route of HNO formation is only important for temperatures between 873 and 1073 K, where the CO oxidation is not efficient.

At high temperatures, from 1173 K and on, NO is also formed through other species than HNO. The most important reaction involve CO_2 (Reaction R22), but HCNO and NH also contribute to the NO formation.

$$CO_2 + N \Leftrightarrow CO + NO \quad \text{(R22)}$$

As at fuel-lean conditions, once NO is formed, some NO–NO_2 interconversion occurs by the reaction of NO with the hydroperoxyl radical (Reaction R10). Though, NO_2 is converted back to NO (Table 3) through reactions with CO (Reaction R11) and H radical (Reaction R12). For temperatures higher than 1123 K all the NO_2 produced is recycled back to NO.

For temperatures higher than 1123 K different reaction paths participate on the NO consumption (Fig. 8). The contribution of the sequence NO → HNO (Reactions R14 and R20) in NO removal is lower than 20 %. It is worth noting that both reactions contribute to the NO production up to 1073 K, as previously detailed. So temperature changes the direction of the reaction. As at fuel-lean conditions, HNO is converted almost completely back to reform NO by reaction with the H atom.

Other important pathway on the NO removal at high temperatures is the route of NO reduction involving ketenyl radicals (Reactions R23 and R24), which results from the interaction of hydrocarbon and nitrogen species. The impact of these reactions on NO consumption increases with temperature. At 1273 K the normalized rate of consumption of NO to form HCNO is equal to −0.321 whereas to form HCN is equal to

NHESSD
1, 7015–7058, 2013

−0.144.

$$HCCO + NO \Leftrightarrow HCNO + CO \quad \text{(R23)}$$

$$HCCO + NO \Leftrightarrow HCN + CO_2 \quad \text{(R24)}$$

The importance of the branching ratio for the HCCO/NO reactions depends on the fate of HCNO (Glarborg et al., 1998). HCNO mostly reforms NO by reacting with oxygenated radicals (Reactions R25 and R26), and produces HCN by reaction with hydrogen atoms (Reaction R27).

$$HCNO + O \Leftrightarrow NO + HCO \quad \text{(R25)}$$

$$HCNO + OH \Leftrightarrow NO + CH_2O \quad \text{(R26)}$$

$$HCNO + H \Leftrightarrow HCN + OH \quad \text{(R27)}$$

In the conditions of this study, the route HCNO → NO prevails over the route HCNO → HCN. At 1273 K where the reactions HCCO + NO (Reactions R23 and R24) are more significant, the normalized rate of consumption of HCNO to form NO (Reactions R25 and R26) is equal to 0.569 while to form HCN (Reaction R27) is equal to 0.425. For lower temperatures the difference between both values is higher.

It is worth noting that even the well known reaction of formation of HCN by means of the reaction of CH_3 and NO (Reaction R28) participates on the HCN production, its contribution on the NO consumption represents less than 5 % of the total NO consumption according to the rate-of-production analysis. Moreover, this reaction is only important at temperatures lower than 1123 K, where neither the production of HCN nor the production of NO are efficient.

$$CH_3 + NO \Leftrightarrow HCN + H_2O \quad \text{(R28)}$$

The sensitivity analysis results at 1073 K (Fig. 9) and 1273 K (Fig. 10) illustrate the complex chemistry of NO at fuel-rich conditions. Results of the sensitivity analysis emphasize the importance of the fate of the hydrocarbon radicals on the NO chemistry.

NHESSD
1, 7015–7058, 2013

The branching reactions leading either to C_2H_6 or CH_2O (CH_3O) enhance the removal or the production of NO, respectively by the subsequent formation of radicals such as HCCO in the case of C_2H_6 (see Fig. 1).

4 NO modelling

4.1 Derivation of the NO global kinetic model

The growing concern for the environment and the increasingly stringent emissions standards in both Europe and the United States have promoted the development of global kinetic mechanisms to study the NO formation in combustion processes, particularly those associated to industrial applications. Thus, the oxidation of NH_3 has been modelled in the simplest way by a two-step scheme (Reactions R29 and R30) as proposed by several authors (De Soete, 1975; Mitchell and Tarbell, 1982).

$$N1 : NH_3 + O_2 \Rightarrow NO + H_2O + \frac{1}{2}H_2 \quad \text{(R29)}$$

$$N2 : NH_3 + NO \Rightarrow N_2 + H_2O + \frac{1}{2}H_2 \quad \text{(R30)}$$

This two-step mechanism represents fairly well the NO chemistry at fuel-lean conditions in relation with the reactions path analysis and the sensitivity analysis. At fuel-rich conditions the sensitization of hydrocarbon radicals and CO/CO_2–NO is more significant. Moreover, the consumption of NO to form HCN through the sequence HCCO (→ HCNO) → HCN acquires more importance as temperature increases.

The number of chemical species and global steps included in the kinetic mechanism must be a balance of the competing needs of accuracy and simplicity to attain the computation time requirements. Moreover, the kinetic model has to be suitable for all different conditions encountered in a wildfire (i.e. both fuel-lean and fuel-rich conditions, different degradation gases composition and temperatures, etc.).

NHESSD
1, 7015–7058, 2013

So, to keep the kinetic mechanism simple we decided to model the NO chemistry from fuel-bound nitrogen by the reaction scheme presented in Reactions (R29) and (R30) and therefore to omit the consumption of NO to form HCN. It is worth noting that this mechanism is only important at fuel-rich conditions and temperatures higher than 1173 K. Moreover, the contribution of this reaction pathway to the consumption of NO varies between 10 % at 1173 K to 28 % at 1273 K, as already detailed in the previous section.

To determine the rate of NH_3 oxidation reaction (Reaction R29) the classical steady-state assumption was used to relate the OH radical to the main components, since the most important reaction on the consumption of ammonia in the conditions of this study is that with the OH radical (Reaction R6). Consequently the OH radical was supposed to be proportional to the square root of the product of O_2 and H_2 concentrations.

Concerning the reaction of NO consumption (Reaction R30), it was assumed that its reaction rate was first order in NH_3 and NO. In addition, due to the different reaction pathways of NO consumption depending on the fuel equivalence ratio, as indicated by the results of the reactions path analysis and previously mentioned, a function of the equivalence ratio was added to the formal expression corresponding to the reaction rate of NO consumption.

Both global mechanisms were coupled without taking into account the possible effects of sensitization of CH_4 and CO/CO_2 to NO.

4.2 Model fitting

The reaction rate expressions of the global model obtained from the calibration are given by Eqs. (1) and (2) being $\dot{\omega}$ is expressed in $\mathrm{mol\,cm^{-3}\,s^{-1}}$.

$$\dot{\omega}_{\{N1\}} = k_{\{N1\}} T^2 \left[NH_3\right]^{1.00} [H_2]^{0.50} [O_2]^{0.50} \exp\left[-\frac{62\,000}{RT}\right] \quad (1)$$

$$\dot{\omega}_{\{N2\}} = k_{\{N2\}} T^{-1.3} \left[NH_3\right]^{1.00} [NO]^{1.00} \exp\left[-\frac{37\,000}{RT}\right] \quad (2)$$

NHESSD
1, 7015–7058, 2013

Where $k_{\{N1\}}$ is equal to 3.22×10^{12} and $k_{\{N2\}}$ is given by Eq. (3).

$$k_{\{N2\}} = \exp\left(45.7 + \Gamma(\varphi - 1) \cdot \varphi^2\right) \quad (3)$$

Where φ is the fuel equivalence ratio and $\Gamma(x)$ is the unit step function (Eq. 4).

$$\Gamma(x) = \begin{cases} 0 & x \leq 0 \\ 1 & x > 0 \end{cases} \quad (4)$$

Figure 11 shows the comparison between the calculated NH_3 and NO concentrations (mole fraction) as a function of the temperature using the global reaction mechanism, and the reference detailed chemistry, for the different fuel equivalence ratios (i.e. 0.6, 1.0 and 1.4).

As it can be seen on this figure, the NO concentration profiles are properly predicted with the global model both at fuel-lean and fuel-rich conditions. The differences between the overall production of NO at 1273 K obtained with the global and the detailed mechanism are 7.4, 11.7, and 12.6 % respectively, for an equivalence ratio of 0.6, 1.0, and 1.4.

Regarding NH_3, there is also a good agreement in general terms between the predicted concentration profiles by the global model and the detailed mechanism. However, the oxidation of NH_3 as a function of the temperature is sharper when predicted by the detailed mechanism GDF-kin® 3.0 than when predicted by the global model, especially at fuel-lean and stoichiometric conditions. As a result the global model is not able to predict the entire consumption of NH_3. The relative errors in the prediction of the global consumption of NH_3 by the global model in comparison with the detailed mechanisms are 14.1, 9.5, and 17.8 % respectively, for an equivalence ratio of 0.6, 1.0, and 1.4.

If the percentage of NH_3 converted into NO is computed, the values obtained with GDF-kin® 3.0 and the global model, are fairly similar (Table 4). The largest divergence

NHESSD
1, 7015–7058, 2013

is observed at fuel-lean conditions, where the global model over predicts the conversion of NH_3–NO because of the error induced by the NH_3 predictions.

Concerning the other major chemical species present in the gases mixture of the degradation gases of vegetation, Figs. 12 and 13 show respectively the CH_4 and O_2; and CO and CO_2 concentrations profiles as a function of the temperature at a fuel equivalence ratio of 1.4. In these conditions, there is a good agreement between the results obtained with both kinetic mechanisms. At stoichiometric and fuel-lean conditions, results show that the predicted temperature at which CH_4, CO, CO_2, and O_2 start being consumed or produced is higher when using the detailed mechanism, as it can be seen on Fig. 14 for the particular case of CH_4 at fuel-lean conditions. The reaction temperature has shifted 50 K due to the sensitization of these species to NO. The discrepancy between the predictions of the global model and the detailed mechanism is only in terms of the temperature of oxidation/production of CH_4, CO, CO_2, and O_2; and since this difference is only about 50 K, predictions of the global model can reasonable be considered as fairly accurate predictions.

5 Discussion

5.1 Model testing

In order to test the model in conditions other than the fitting conditions, the model was tested for another residence time (i.e. 0.6 s) representative of the conditions encountered during a wildfire.

Figure 15 presents the results of the calculated NH_3 and NO concentrations (mole fraction) as a function of the temperature by using the global model and the reference detailed mechanism at fuel-lean and fuel-rich conditions, corresponding to fuel equivalence ratios of 0.6 and 1.4 respectively. As it can be seen on this figure, the NO concentration profiles are accurately predicted with the global model. The differences between the overall production of NO at 1273 K obtained with the global and the detailed mechanisms are 2.0 and 4.3 % respectively, for an equivalence ratio of 0.6 and 1.4.

NHESSD
1, 7015–7058, 2013

Concerning NH_3, as for a residence time of 1.3 s, even though there is also a general good agreement between the predicted concentration profiles by the global model and the detailed mechanism, the concentration of NH_3 as a function of the temperature drops sharply when predicted by the detailed mechanism than when predicted by the global model. Thus, the global model is not able to predict the entire consumption of NH_3. In this case, the relative errors in the predictions of the global NH_3 consumption by the global model in comparison with the detailed mechanisms are respectively for an equivalence ratio of 0.6 and 1.4, 20.6 % and 22.0 %.

Conversion factors of NH_3 to NO computed by the values obtained with the global model are 37.3 % and 4.7 % for fuel-lean and fuel-rich conditions respectively. The corresponding values obtained with the detailed kinetic mechanism are 29 % and 3.5 %. As for a residence time of 1.3 s, the observed differences between prediction with the global model and the detailed kinetic mechanism are due to the error in the prediction of the entire consumption of NH_3 by the global model.

For the other major chemical species present in the gases mixture of the degradation gases of vegetation, CH_4, O_2, CO and CO_2, the concentrations profiles as a function of the temperature are properly predicted at either fuel-lean and fuel-rich conditions. In this case no shift of the reaction temperature is produced as it was observed for a residence time of 1.3 s. Thus, the NO global model coupled to the CH_4/CO model captures the essential features of the NO chemistry.

5.2 Comparison to experimental data available in the literature

To our knowledge, there are no experimental data in the literature concerning the NO formation in PSR devices for $CH_4/CO/CO_2/NH_3$ gases mixtures in the conditions of this study. The experimental study performed in a PSR device that presents conditions close to the present work is that of Dagaut et al. (1998). The experimental data of this work was used to develop the model for the NO chemistry included in the detailed mechanism of reference. Therefore, comparing our results with these data will not actually provide new information.

NHESSD
1, 7015–7058, 2013

Thus, in order to backup at least in the order of magnitude the present results with experimental data, we have compared the results of this work in terms of NH_3 conversion to NO with the work of Mendiara and Glarborg (2009).

Mendiara and Glarborg (2009) studied the ammonia chemistry in the oxy-fuel combustion of methane. Experiments were performed in a flow reactor at temperatures ranging between 973 and 1773 K, at different fuel equivalence ratios and for CH_4/NH_3 mixtures highly diluted in CO_2 or N_2. The residence time in the reactor was of the order of 1 s.

According to their results, conversion factors of NH_3 to NO strongly depend on the presence of CO_2 in the mixture. For CH_4/NH_3 mixtures diluted in CO_2, the conversion of NH_3 to form NO varied between 27 % at fuel-lean conditions to 15 % at fuel-rich conditions. For CH_4/NH_3 mixtures diluted in N_2 these values were 47 and 4 % respectively. Thus, as stated by Mendiara and Glarborg (2009), CO_2 enhances the formation of NO under fuel-rich conditions while it inhibits the NO formation under stoichiometric and fuel-lean conditions.

The corresponding values predicted by the global model varied between 28.5 % at fuel-lean conditions and 2.4 % at fuel-rich conditions for a residence time of 1.3 s, and between 37.3 and 4.7 % for a residence time of 0.6 s.

The results obtained with the two-step global mechanisms are consistent with the experimental data, especially concerning the simulations run for a residence time of 1.3 s which is a value closer to the conditions in which experimental data were obtained. However, a major difference is observed at fuel-rich conditions, since a greater amount of NO formation would be expected according to the experimental data of Mendiara and Glarborg (2009). Clearly, the high content of CO present in the gaseous mixture of degradation gases, but not in the mixture studied by Mendiara and Glarborg (2009), and the derived sensitization effects to CH_4 and NO are responsible for this divergence. According to Glarborg and Bentzen (2008) high concentrations of CO in the oxidation of CH_4 led to alterations in the amount and partitioning of O/H radicals with implications on the NH_3 conversion.

NHESSD
1, 7015–7058, 2013

6 Conclusions

NO emissions from the combustion of vegetation at the source level have been studied numerically, considering that the volatile fraction of fuel-N released due to the thermal degradation of vegetation is composed by NH_3. The main chemical pathways and their occurrence depending on the conditions of this study have been established. NO is mainly produced through the sequence $NH_3 \rightarrow NH_2$ ($\rightarrow H_2NO$) $\rightarrow HNO \rightarrow NO$ ($\leftrightarrow NO_2$). However, at fuel-rich conditions NO chemistry is more complex and a larger number of chemical species and thus reaction pathways are involved in the processes of NO formation and consumption. Moreover, in these conditions the effects of sensitization of hydrocarbons and CO/CO_2 to NO are more significant.

According to the reactions path analysis through rate-of-production and the sensitivity analyses a two-step global kinetic model has been proposed for the oxidation of ammonia. The obtained mechanism succeeds in predicting the final concentrations of NO and $NH_3$with reasonable accuracy in comparison with the numerical values obtained with the detailed kinetic mechanism GDF-Kin® 3.0 for different conditions in terms of temperatures, fuel equivalence ratio and residence time.

Different fuels containing CH_4, CO, CO_2, and NH_3 could be studied with the coupling of the two-step mechanism developed herein and the five-step mechanism for CH_4/CO.

Acknowledgements. This research was supported by the French National Research Agency (ANR), under the project ANR-09-COSI-006 and by the French National Center for Scientific Research (CNRS).

References

Barboni, T., Cannac, M., Pasqualini, V., Simeoni, A., Leoni, E., and Chiaramonti, N.: Volatile and semi-volatile organic compounds in smoke exposure of firefighters during prescribed burning in the Mediterranean region, Int. J. Wildland Fire, 19, 606–612, 2010.

NHESSD
1, 7015–7058, 2013

Bartok, W., Engleman, V. S., Goldstein, R., and del Valle, E. G.: Basic kinetic studies and modeling of nitrogen oxide formation in combustion processes, AICHE Sym. S., 126, 30–38, 1972.

Brink, A., Boström S., Kilpinen, P., and Hupa, M.: Modeling nitrogen chemistry in the freeboard of biomass-FBC, IFRF Combustion Journal, 1–14 200107, 2001.

Dagaut, P., Lecomte, F., Chevailler, S., and Cathonnet, M.: Experimental and detailed kinetic modeling of nitric oxide reduction by a natural gas blend in simulated reburning conditions, Combust. Sci. Technol., 139, 329–363, 1998.

David, R. and Matras, D.: Règles de construction et d'extrapolation des réacteurs auto-agités par jets gazeux, Can. J. Chem. Eng., 53, 297–300, 1975 (in French).

De Soete, G. G.: Overall reaction rates of NO and N_2 formation from fuel nitrogen, P. Combust. Inst., 15, 1093–1102, 1975.

Duterque, J., Avezard, N., and Borghi, R.: Further results on nitrogen oxides production in combustion, zones, Combust. Sci. Technol., 25, 85–89, 1981.

El Bakali, A., Dagaut, P., Pillier, L., Desgroux, P., Pauwels, J. F., Rida, A., and Meunier, P.: Experimental and modeling study of the oxidation of natural gas in a premixed flame, shock tube and jet-stirred reactor, Combust. Flame, 137, 109–128, 2004.

El Bakali, A., Pillier, L., Desgroux, P., Lefort, B., Gasnot, L., Pauwels, J. F., and da Costa, L.: NO prediction in natural gas flames using GDF-Kin®3.0 mechanism NCN and HCN contribution to prompt-NO formation, Fuel, 85, 896–909, 2006.

Faravelli, T., Frassoldati, A., and Ranzi, E.: Kinetic modeling of the interactions between NO and hydrocarbons in the oxidation of hydrocarbons at low temperatures, Combust. Flame, 132, 188–207, 2003.

Glarborg, P.: Hidden interactions – Trace species governing combustion and emissions, P. Combust. Inst., 31, 77–98, 2007.

Glarborg, P. and Bentzen, L. L. B.: Chemical effects of high CO_2 concentration in oxy-fuel combustion of methane, Energ. Fuel., 22, 291–296, 2008.

Glarborg, P., Kee, R. J., Grcar, J. F., and Miller, J. A.: PSR: a FORTRAN program for modeling well-stirred reactors, Report No. SAND 86-8209, Sandia National Laboratories, Albuquerque, NM, 1986.

Glarborg, P., Alzueta, M. U., Dam-Johansen, K., and Miller, A.: Kinetic modeling of hydrocarbon/nitric oxide interactions in a flow reactor, Combust. Flame, 115, 1–27, 1998.

NHESSD

1, 7015–7058, 2013

Grewe, V., Dahlmann, K., Matthes, S., and Steinbrecht, W.: Attributing ozone to NO_x emissions: implications for climate mitigation measures, Atmos. Environ., 59, 102–107, 2012.
Jaffe, D. A. and Widger, N. L.: Ozone production from wildfires: a critical review, Atmos. Environ., 51, 1–10, 2012.
Jallais, S.: Etude expérimentale et modélisation de l'oxydation d'hydrocarbures légers, Ph.D. thesis, ENSMA, Poitiers, 2001 (in French).
Kee, R. J., Rupley, F. M., and Miller, J. A.: CHEMKIN-II: a FORTRAN chemical kinetics package for the analysis of gas-phase chemical kinetics, Report No. SAND 89-8009, Sandia National Laboratories, Livermore, CA, USA, 1989.
Leroy, V., Leoni, E., and Santoni, P. A.: Reduced mechanism for the combustion of evolved gases in forest fires, Combust. Flame, 154, 410–433, 2008.
Mebust, A. K., Russell, A. R., Hudman, R. C., Valin, L. C., and Cohen, R. C.: Characterization of wildfire NO_x emissions using MODIS fire radiative power and OMI tropospheric NO_2 columns, Atmos. Chem. Phys., 11, 5839–5851, doi:10.5194/acp-11-5839-2011, 2011.
Mendiara, T. and Glarborg, P.: Ammonia chemistry in oxy-fuel combustion of methane, Combust. Flame, 156, 1937–1949, 2009.
Miller, J. and Bowman, C.: Mechanism and modeling of nitrogen chemistry in combustion, Prog. Energ. Combust., 15, 287–338, 1989.
Miranda, A. I.: An integrated numerical system to estimate air quality effects of forest fires, Int. J. Wildland Fire, 13, 1–10, 2004.
Mitchell, J. W. and Tarbell, J. M.: A kinetic model of nitric oxide formation during pulverized coal combustion, AICHE J., 28, 302–311, 1982.
Morvan, D. and Dupuy, J. L.: Modelling the propagation of a wildfire through a Mediterranean shrub using a multiphase Formulation, Combust. Flame, 138, 199–210, 2004.
Ottomar, R., Miranda, A. I., and Sandberg, D.: Characterizing sources of emissions from wildland fires, Chapter 3, in: Wildland Fires and Air Pollution, Developments in Environmental Science, edited by: Bytnerowicz, A., Arbaugh, M., Riebau, A., and Andersen, C., vol. 8, Elsevier, Amsterdam, ISBN 978-0-08–055609-3, 2009.
Pérez-Ramirez, Y., Santoni, P. A., Darabiha, N., Leroy-Cancellieri, V., and Leoni, E.: A global kinetic model for the combustion of the evolved gases in wildland fires, Combust. Sci. Technol., 184, 1380–1394, 2012.

NHESSD
1, 7015–7058, 2013

Rogaume, T., Koulidiati, J., Richard, F., Jabouille, F., and Torero, J.: A model of the chemical pathways leading to NO_x formation during combustion of mixtures of cellulosic and plastic materials, Int. J. Therm. Sci., 45, 359–366, 2006.

Salzmann, R. and Nussbaumer, T.: Fuel staging for NO_x reduction in biomass combustion: experiments and modeling, Energ. Fuel., 15, 575–582, 2001.

Santoni, P. A.: Introduction à la problématique des feux de forêt, Ecole de combustion, Ecole thématique du CNRS, Fréjus, France, 2008 (in French).

Santoni, P. A., Simeoni, A., Rossi, J. L., Bosseur, F., Morandini, F., Silvani, X., Balbi, J. H., Cancellieri, D., and Rossi, L.: Instrumentation of wildland fire: characterization of a fire spreading through a Mediterranean shrub, Fire Safety J., 41, 171–184, 2006.

Strada, S., Mari, C., Filippi, J.-B., and Bosseur, F.: Wildfire and the atmosphere: modelling the chemical and dynamic interactions at the regional scale, Atmos. Environ., 51, 234–249, 2012.

Sullivan, A. L.: A review of wildland fire spread modelling, 1990–present, 1. Physical and quasi-physical models, Int. J. Wildland Fire, 18, 349–368, 2009.

Sullivan, A. L. and Ball, R.: Thermal decomposition and combustion chemistry of cellulosic biomass, Atmos. Environ., 47, 133–141, 2012.

Sullivan, N., Jensen, A., Glarborg, P., Day, M. S., Grcar, J. F., Bell, J. B., Pope, C. J., and Kee, R. J.: Ammonia conversion and NO_x formation in laminar coflowing nonpremixed methane-air flames, Combust. Flame, 131, 285–298, 2002.

Tihay, V., Santoni, P. A., Simeoni, A., Garo, J. P., and Vantelon, J. P.: Skeletal and global mechanisms for the combustion of gases released by crushed forest fuels, Combust. Flame, 156, 1565–1575, 2009a.

Tihay, V., Simeoni, A., Santoni, P. A., Rossi, L., Garo, J. P., and Vantelon, J. P.: Experimental study of laminar flames obtained by the homogenization of three forest fuels, Int. J. Therm. Sci., 48, 488–501, 2009b.

Weissinger, A., Fleckl, T., and Obernberger, I.: In situ FT-IR spectroscopic investigations of species from biomass fuels in a laboratory-scale combustor: the release of nitrogenous species, Combust. Flame, 137, 403–417, 2004.

Zhou, H., Jensen, A., Glarborg, P., and Kavaliauskas, A.: Formation and reduction of nitric oxide in fixed-bed combustion of straw, Fuel, 85, 705–716, 2006.

NHESSD

1, 7015–7058, 2013

Table 1. Reaction rate equations and parameters of the global kinetic mechanism (φ: equivalence ratio; units $\dot{\omega}$: mol cm^{-3} s^{-1}, E: cal mol^{-1}, k: consistent units) (Pérez-Ramirez et al., 2012).

Reaction rate equation	Parameters
$\dot{\omega}_{R1} = k_{\{R1\}}[CH_4]^{-0.33}[O_2]^{1.0}\left([CH_3]+[CH_2O]\right)^{0.85}\exp\left[-\frac{E_{\{R1\}}}{RT}\right]$	$k_{\{R1\}} = \exp(27.85+0.25\varphi)$ $E_{\{R1\}} = 41\,670$
$\dot{\omega}_{R2} = k_{\{R2\}}[CH_3]^{0.94}[O_2]^{0.66}\exp\left[-\frac{E_{\{R2\}}}{RT}\right]$	$k_{\{R2\}} = 1.07\times10^{12}$ $E_{\{R2\}} = 36\,002$
$\dot{\omega}_{R3} = k_{\{R3\}}[CH_2O]^{1.11}[O_2]^{0.38}\exp\left[-\frac{E_{\{R3\}}}{RT}\right]$	$k_{\{R3\}} = 1.06\times10^{13}$ $E_{\{R3\}} = 41\,976$
$\dot{\omega}_{R4f} = k_{\{R4f\}}[H_2]^{1.00}[O_2]^{0.50}\exp\left[-\frac{E_{\{R4f\}}}{RT}\right]$	$k_{\{R4f\}} = 2.90\times10^{13}$ $E_{\{R4f\}} = 48\,484$
$\dot{\omega}_{R4r} = k_{\{R4r\}}[H_2O]^{1.00}\exp\left[-\frac{E_{\{R4r\}}}{RT}\right]$	$k_{\{R4r\}} = 3.93\times10^{12}$ $E_{\{R4r\}} = 106\,058$
$\dot{\omega}_{R5f} = k_{\{R5f\}}[CO]^{1.00}[O_2]^{0.50}\exp\left[-\frac{E_{\{R5f\}}}{RT}\right]$	$k_{\{R5f\}} = \exp(33.40-3.50\varphi)$ $E_{\{R5f\}} = 47\,773$
$\dot{\omega}_{R5r} = k_{\{R5r\}}[CO_2]^{1.00}\exp\left[-\frac{E_{\{R5r\}}}{RT}\right]$	$k_{\{R5r\}} = 2.90\times10^{13}$ $E_{\{R5r\}} = 112\,042$

NHESSD
1, 7015–7058, 2013

Table 2. Normalized rate-of-production or normalized rate-of-consumption (negative values) of NO_2 as a function of the temperature at fuel-lean conditions.

Reaction	Normalized rates of production or consumption of NO_2										
	773 K	823 K	873 K	923 K	973 K	1023 K	1073 K	1123 K	1173 K	1223 K	1273 K
$NO+HO_2 \leftrightarrow NO_2+OH$	1.00	1.00	1.00	0.99	0.97	0.85	0.93	0.96	0.96	0.93	0.89
$NO_2+HO_2 \leftrightarrow HONO+O_2$	−0.45	−0.40	−0.28	−0.19	−0.18	−0.27	−0.07	–	–	–	–
$NO_2+CO \leftrightarrow NO+CO_2$	−0.52	−0.55	−0.64	−0.67	−0.60	−0.33	–	–	–	–	–
$NO_2+H \leftrightarrow NO+OH$	–	–	–	−0.07	−0.13	−0.30	−0.80	−0.76	−0.68	−0.61	−0.56
$NO_2+O \leftrightarrow NO+O_2$	–	–	–	–	–	–	−0.12	−0.20	−0.30	−0.38	−0.43

NHESSD
1, 7015–7058, 2013

Table 3. Normalized rate-of-production or normalized rate-of-consumption (negative values) of NO_2 as a function of the temperature at fuel-rich conditions.

Reaction	Normalized rates of production or consumption of NO_2										
	773 K	823 K	873 K	923 K	973 K	1023 K	1073 K	1123 K	1173 K	1223 K	1273 K
$NO+HO_2 \leftrightarrow NO_2+OH$	1.00	1.00	1.00	1.00	1.00	1.00	1.00	0.99	0.99	0.99	0.99
$NO_2+CO \leftrightarrow NO+CO_2$	−0.86	−0.87	−0.91	−0.93	−0.93	−0.90	−0.81	–	–	–	–
$NO_2+H \leftrightarrow NO+OH$	–	–	–	–	–	–	−0.10	−0.98	−0.99	−0.99	−0.99

NHESSD
1, 7015–7058, 2013

Table 4. Percentage of NH_3 conversion to NO.

φ	GDF-kin® 3.0	2-steps global model
0.6	22.8	28.5
1.0	18.1	19.8
1.4	2.3	2.4

NHESSD
1, 7015–7058, 2013

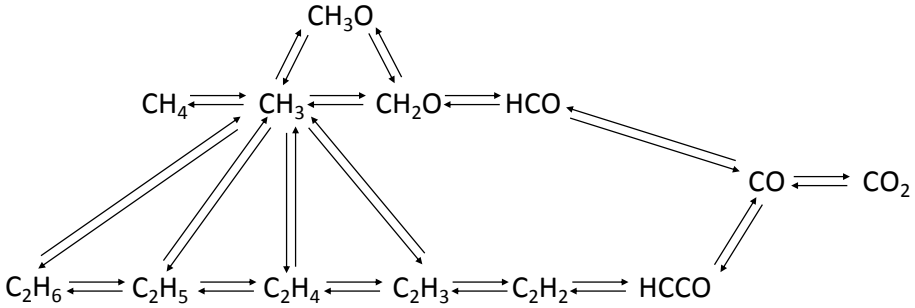

Fig. 1. Reaction pathways for the combustion of methane.

NHESSD
1, 7015–7058, 2013

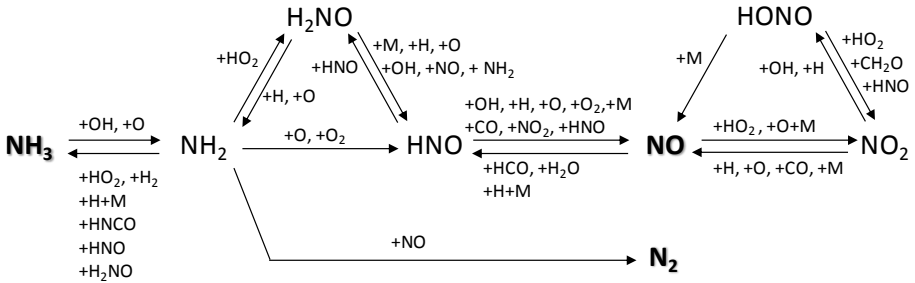

Fig. 2. Reaction paths diagram of the principal reactions involved on the NO chemistry at fuel-lean conditions.

NHESSD
1, 7015–7058, 2013

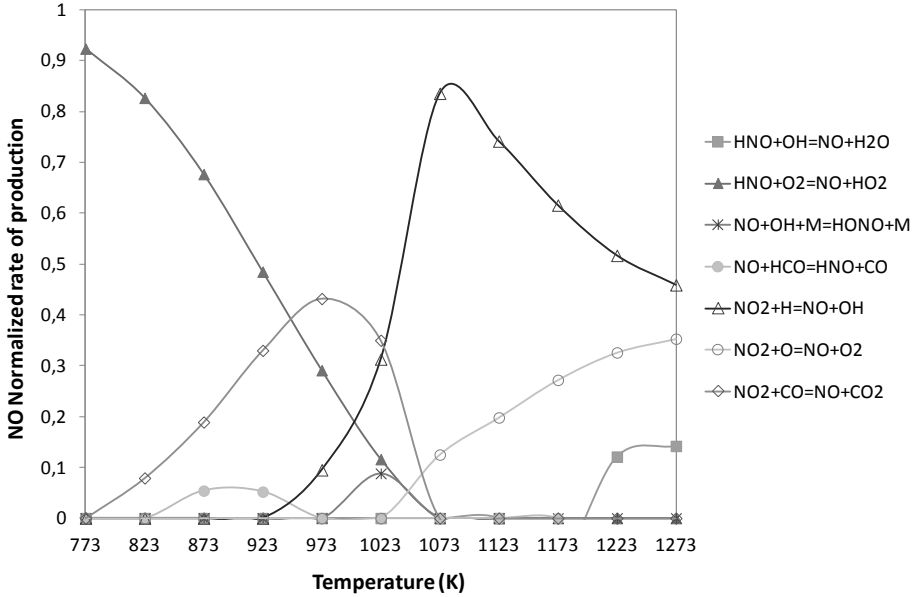

Fig. 3. Normalized rate of production of NO at fuel-lean conditions (φ = 0.6).

NHESSD
1, 7015–7058, 2013

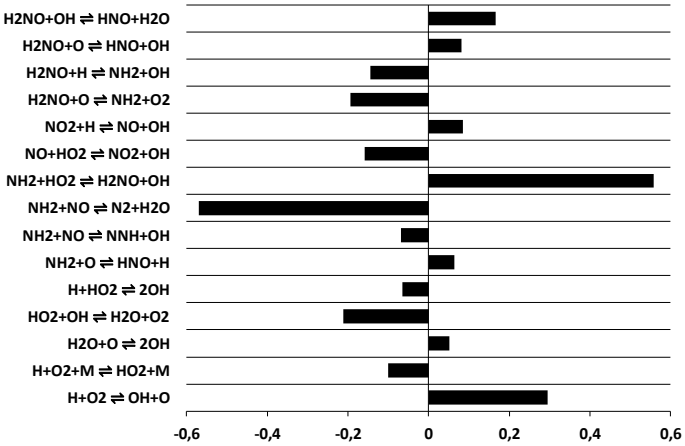

Fig. 4. PSR code outputs for sensitivity analysis on NO at fuel-lean conditions ($\varphi = 0.6$) and 1073 K.

NHESSD
1, 7015–7058, 2013

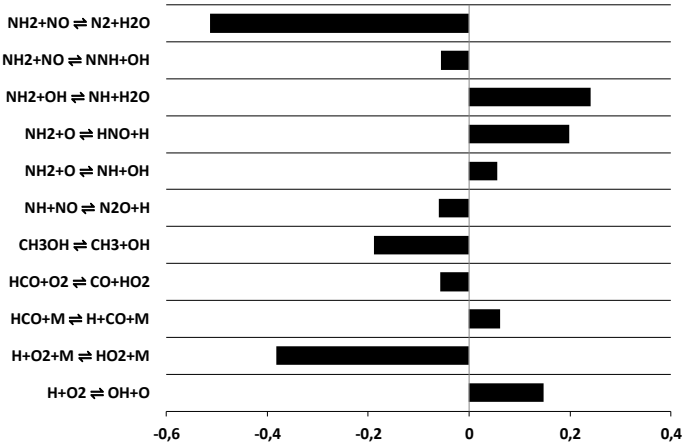

Fig. 5. PSR code outputs for sensitivity analysis on NO at fuel-lean conditions ($\varphi = 0.6$) and 1273 K.

NHESSD
1, 7015–7058, 2013

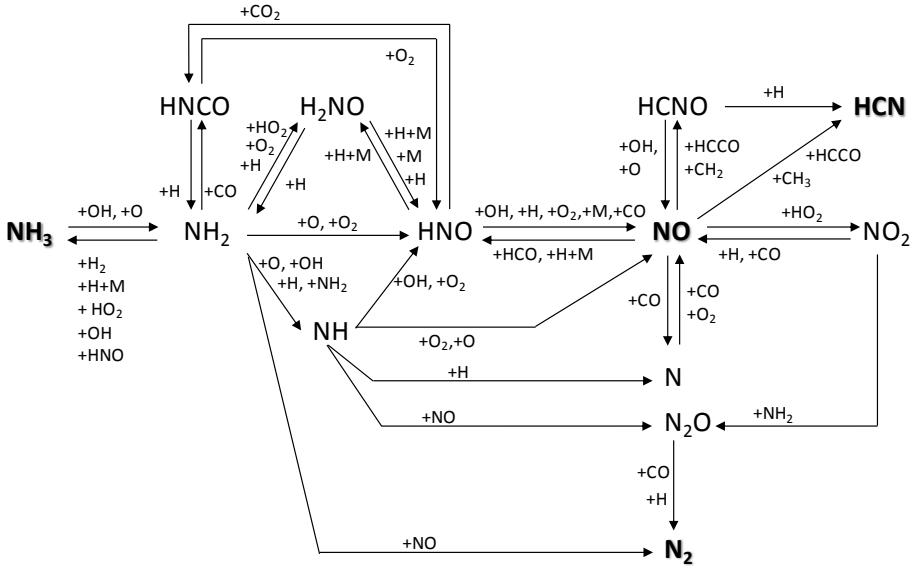

Fig. 6. Reaction paths diagram of the principal reactions involved on the NO chemistry at fuel-rich conditions.

NHESSD
1, 7015–7058, 2013

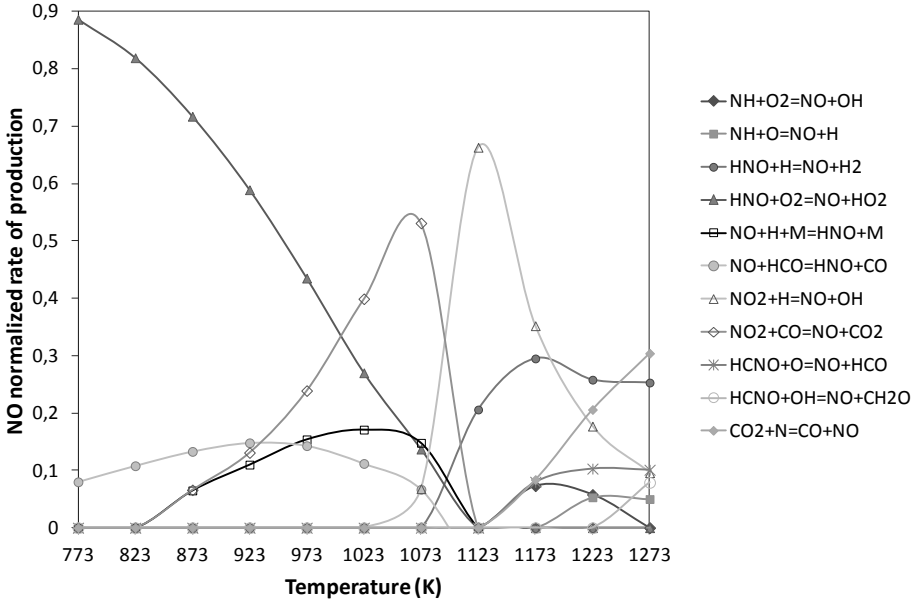

Fig. 7. Normalized rate of production of NO at fuel-rich conditions (φ = 1.4).

NHESSD
1, 7015–7058, 2013

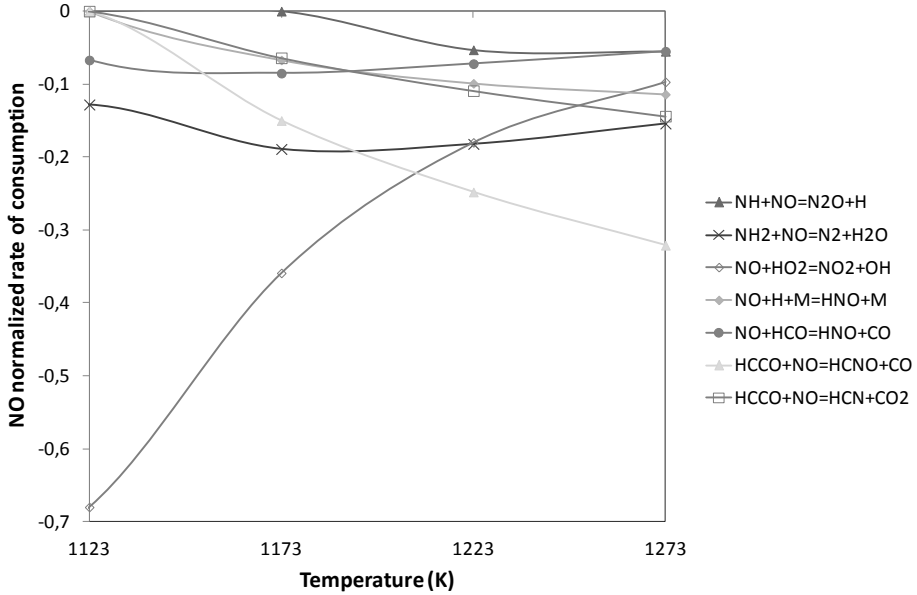

Fig. 8. Normalized rate of consumption of NO at fuel-rich conditions (φ = 1.4).

NHESSD
1, 7015–7058, 2013

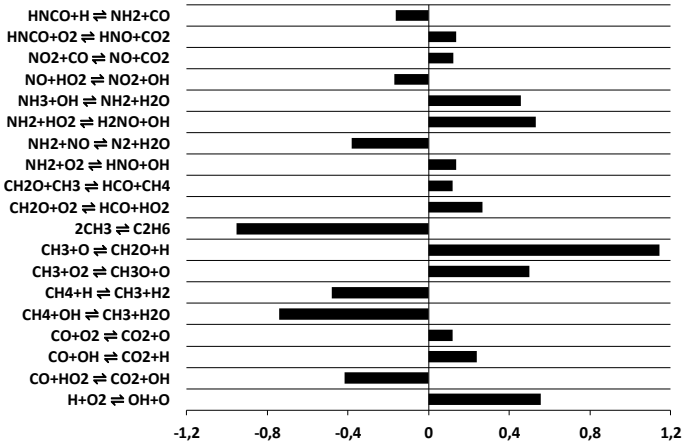

Fig. 9. PSR code outputs for sensitivity analysis on NO at fuel-rich conditions ($\varphi = 1.4$) and 1073 K.

NHESSD
1, 7015–7058, 2013

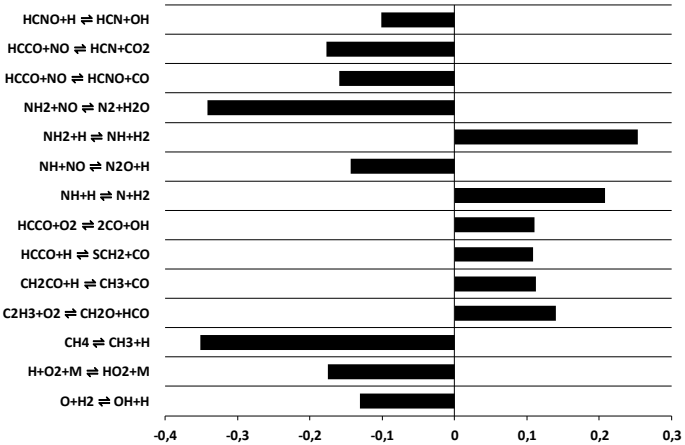

Fig. 10. PSR code outputs for sensitivity analysis on NO at fuel-rich conditions (φ = 1.4) and 1273 K.

NHESSD
1, 7015–7058, 2013

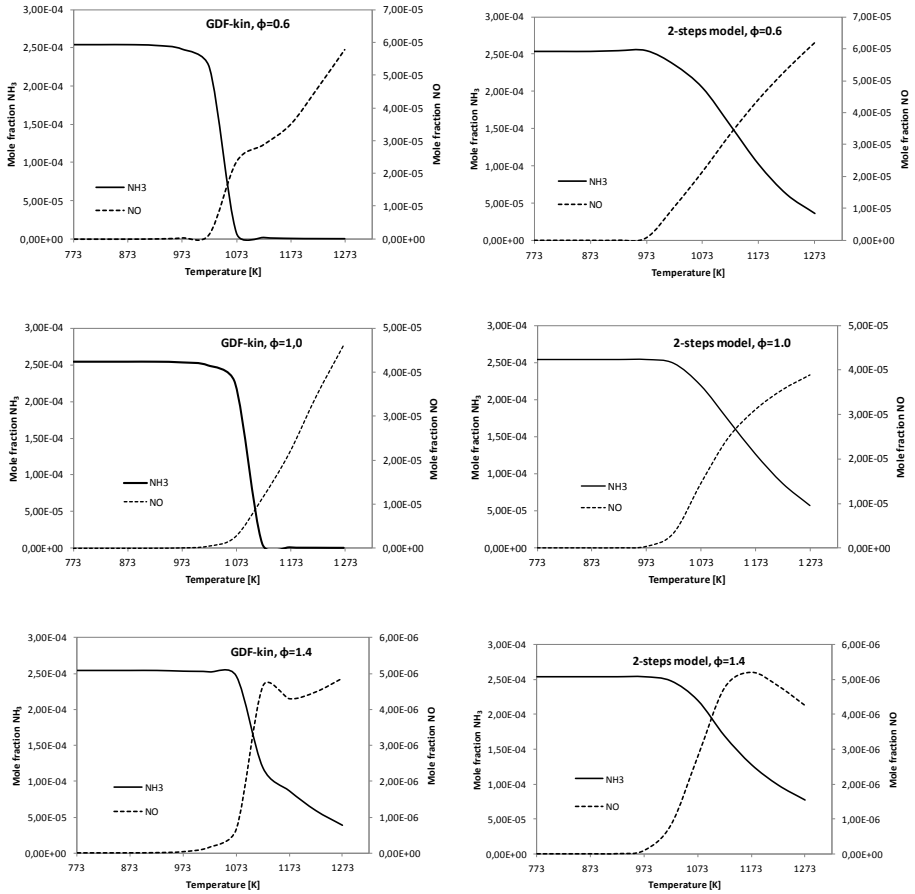

Fig. 11. Comparison between the NO and NH_3 mole fractions concentrations obtained with the detailed mechanism GDF-Kin® 3.0 and the global model developed in the present work as a function of the temperature, and for different equivalence ratios (i.e. φ = 0.6, 1.0 and 1.4), for a residence time of 1.3 s.

NHESSD
1, 7015–7058, 2013

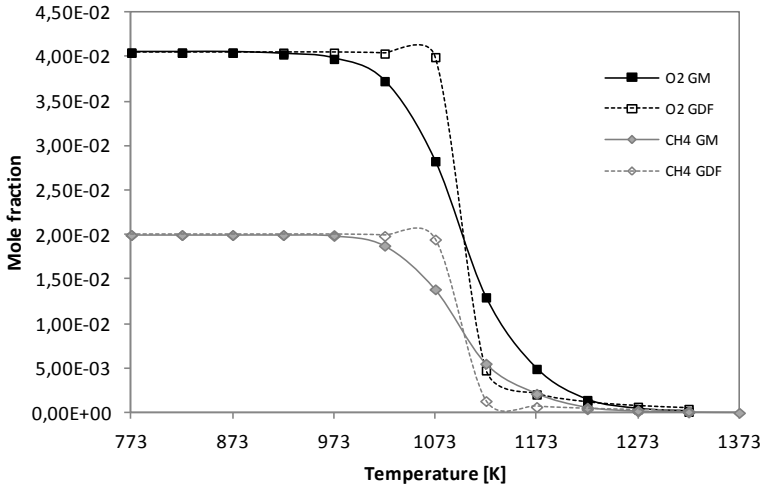

Fig. 12. Comparison between the CH_4 and O_2 mole fractions concentrations obtained with the detailed mechanism GDF-Kin® 3.0 (GDF on the legend) and the global model (GM on the legend) as a function of the temperature at fuel-rich conditions.

NHESSD
1, 7015–7058, 2013

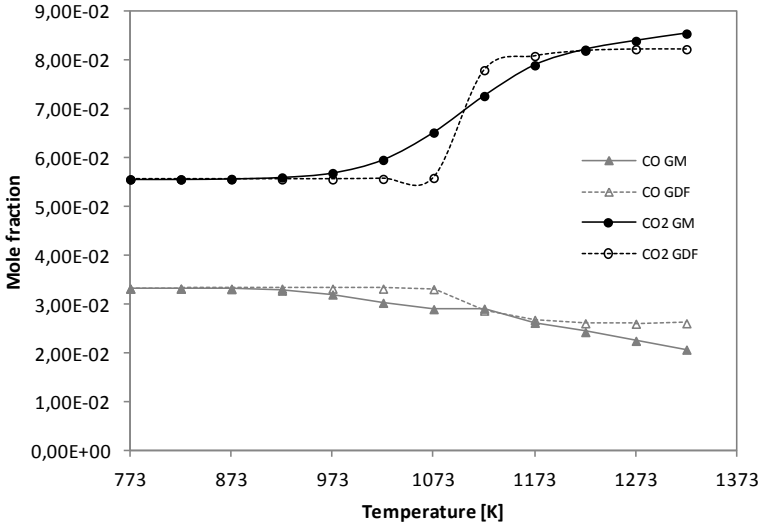

Fig. 13. Comparison between the CO and CO_2 mole fractions concentrations obtained with the detailed mechanism GDF-Kin® 3.0 (GDF on the legend) and the global model (GM on the legend) as a function of the temperature at fuel-rich conditions.

NHESSD
1, 7015–7058, 2013

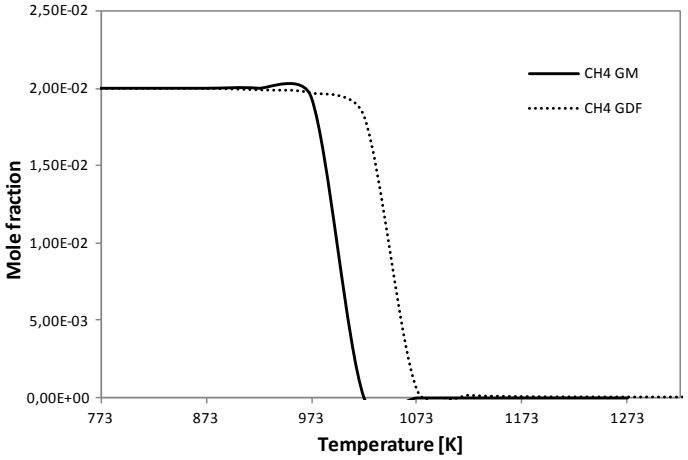

Fig. 14. Comparison between the CH_4 mole fractions concentrations obtained with the detailed mechanism GDF-Kin® 3.0 (GDF on the legend) and the global model (GM on the legend) as a function of the temperature at fuel-lean conditions.

NHESSD
1, 7015–7058, 2013

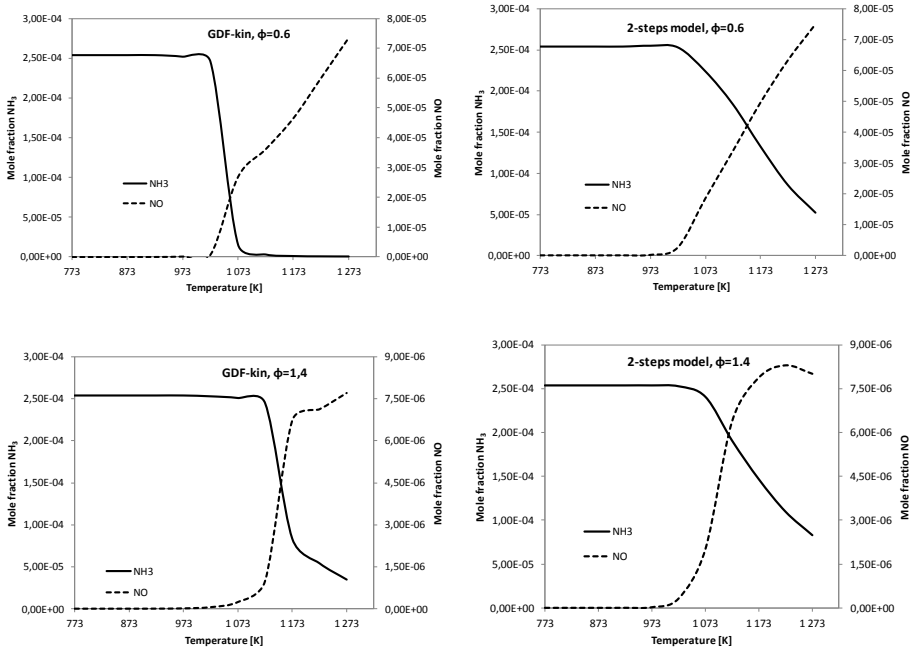

Fig. 15. Comparison between the NO and NH_3 mole fractions concentrations obtained with the detailed mechanism GDF-Kin® 3.0 and the global model developed in the present work as a function of the temperature, and for different equivalence ratios (i.e. φ = 0.6 and 1.4), for a residence time of 0.6 s.

NHESSD
1, 7015–7058, 2013